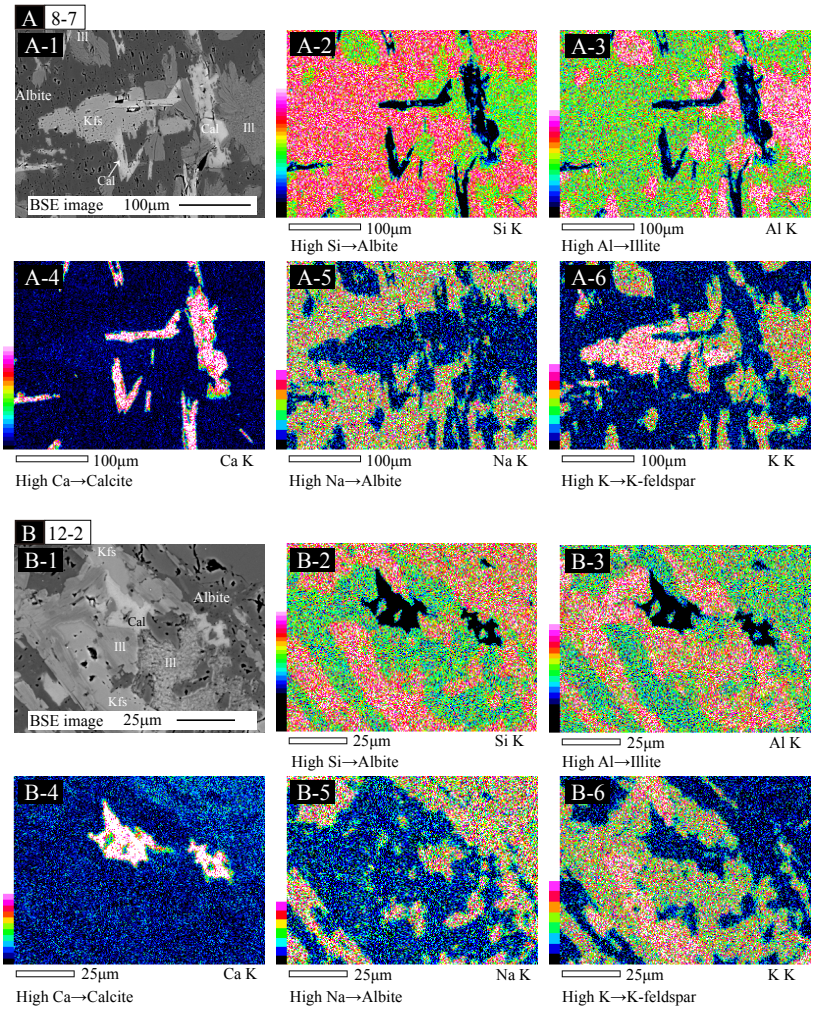

SUPPLEMENTARY FIGURE S1. BSE images (A-1 and B-1) and chemical maps showing the elemental Si, Al, Ca, Na, and K concentrations (A-2 to A-6 and B-2 to B-6) of samples No. 8-7 and No. 12-2. High concentrations are indicated by warm colors and low concentrations by cold colors. Illite, calcite, albite, and K-feldspar can be identified by the high concentrations of elemental Al, Ca, Na, and K, respectively.

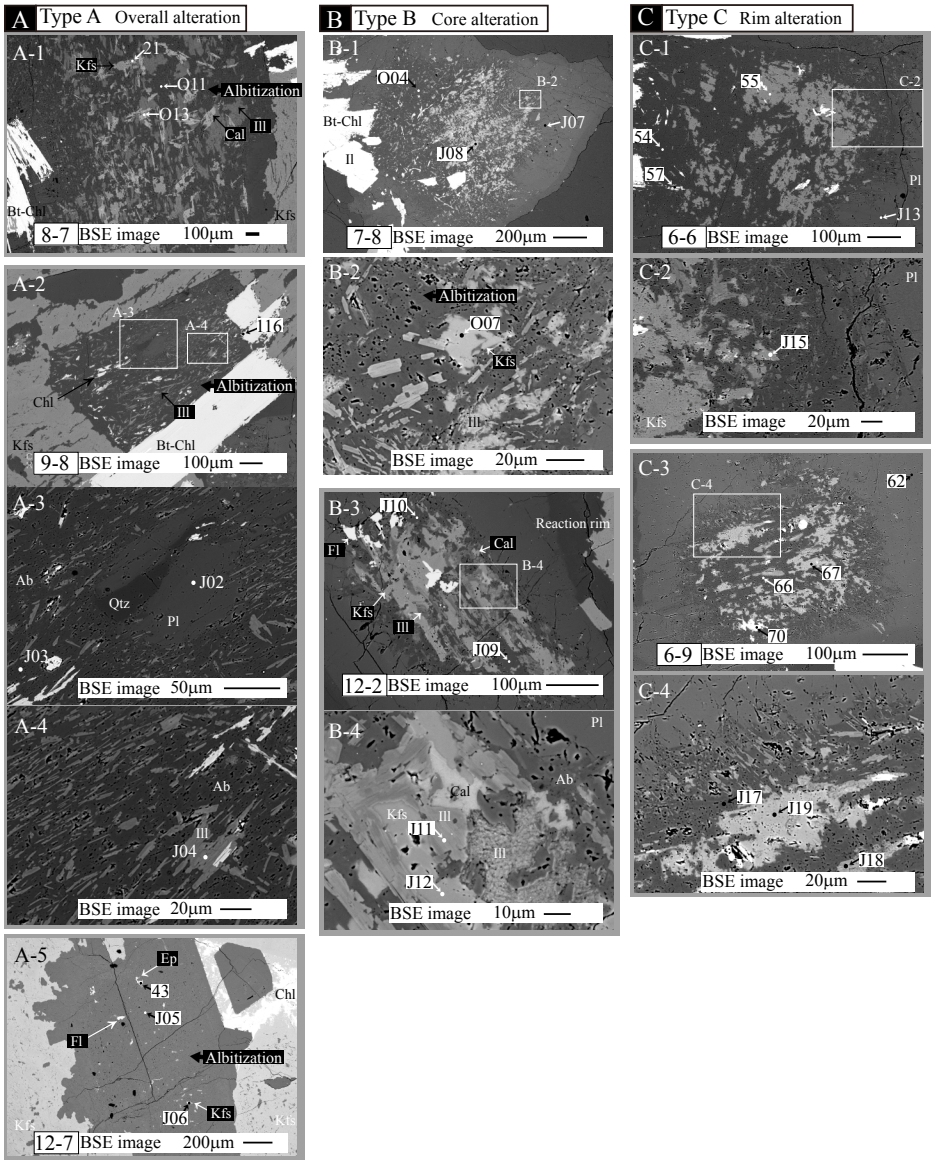

SUPPLEMENTARY FIGURE S2. BSE images of the altered Types A, B, and C plagioclases and the analysis points used to obtain their chemical compositions. The numbers correspond to the analysis points listed in Table 1 and S1.

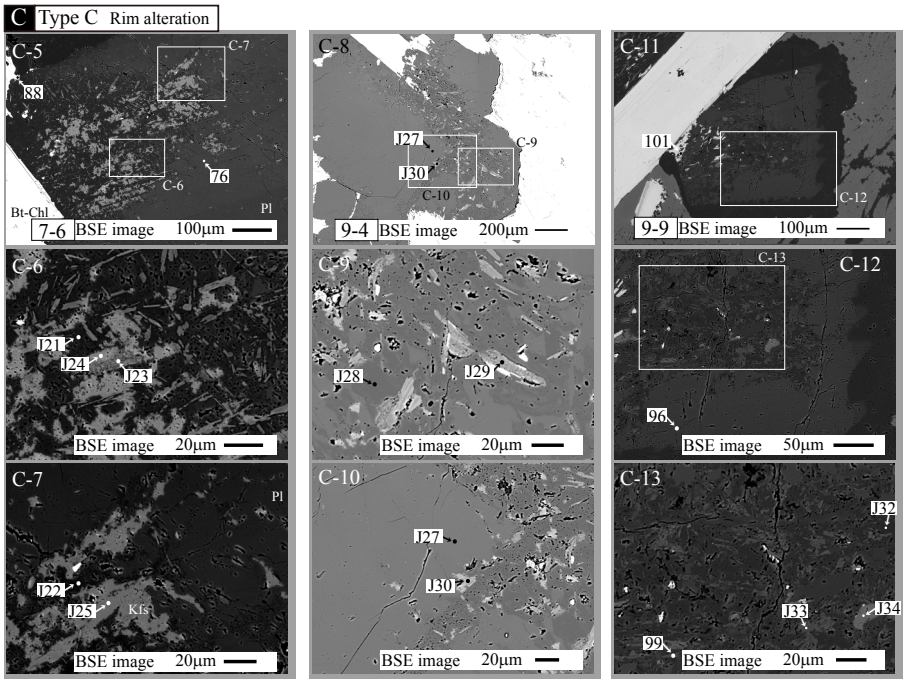

Supplementary Figure S2 (continued). BSE images of the altered Types A, B, and C plagioclases and the analysis points used to obtain their chemical compositions. The numbers correspond to the analysis points listed in Table 1 and S1.

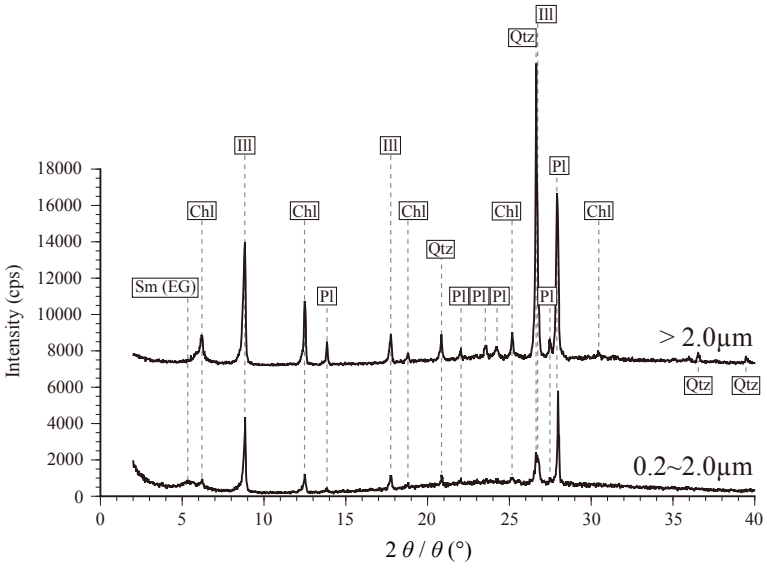

Supplementary Figure S3. XRD pattern of the 0.2–2.0 μm and >2.0 μm powder samples separated from the plagioclase of sample no. 06MI03-8, crystallographically confirming the occurrence of illite.

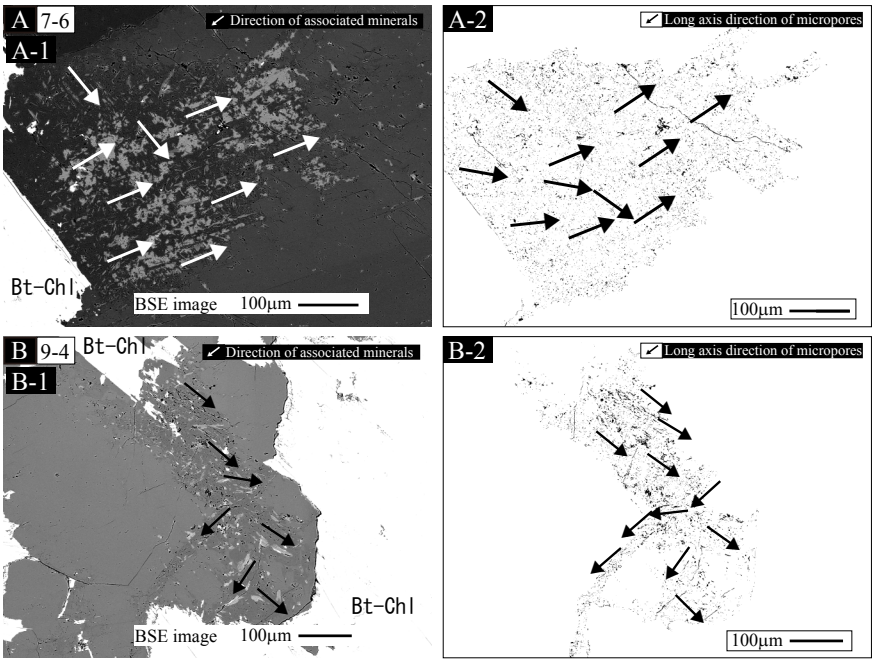

Supplementary Figure S4. Direction of the associated minerals and the long axis direction of micropores in the alteration area of samples no. 7-6 (A) and 9-4 (B). Arrows indicate the direction of mass transfer from the chlorite into the plagioclase.

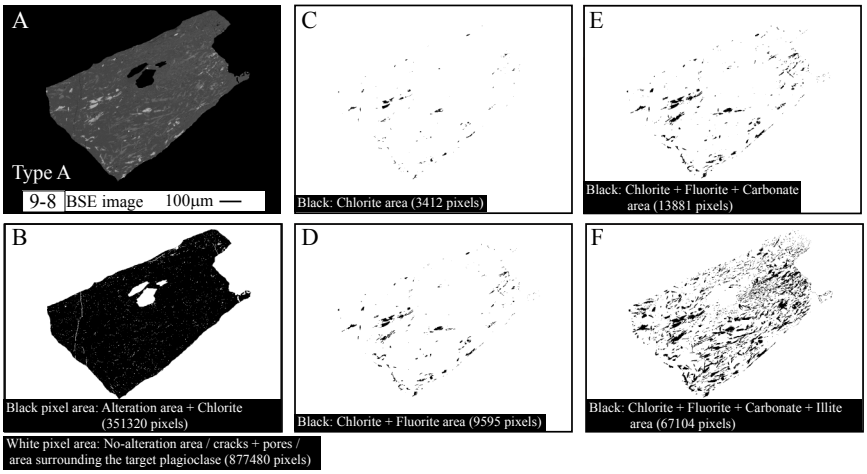

Supplementary Figure S5. Image analysis revealing the volume (areal) ratios of the alteration minerals obtained using image processing software, with sample No. 9-8 as an example. (A) The alteration area containing the micropores was clipped from the BSE image using the image processing software Photoshop®. (B) The binary image processing using the Scion image software divided the image into black pixels, which includes the alteration area and chlorite (351,320 pixels), and white pixels, which corresponded to the unaltered area, micropores, microcracks, and areas other than the target alteration area (877,480 pixels). (C) Chlorite (3,412 pixels), giving an alteration area of 347,908 (351,320 - 3,412) pixels. (D) Sum of chlorite and fluorite (9,595 pixels), giving a fluorite count of 6,183 (9,595 - 3,412) pixels. (E) Sum of chlorite, fluorite, and calcite (13,881 pixels), giving a calcite pixel count of 4,286 (13,881 - 9,595) pixels. (F) Sum of chlorite, fluorite, calcite, and illite (67,104 pixels), giving an illite count of 53,223 (67,104 - 13,881) pixels. The pixel count of albite was determined subtracting chlorite, fluorite, calcite, and illite (67,104 pixels) the alteration area (347,908 pixels), giving an albite count of 280,804 pixels for sample No. 9-8.

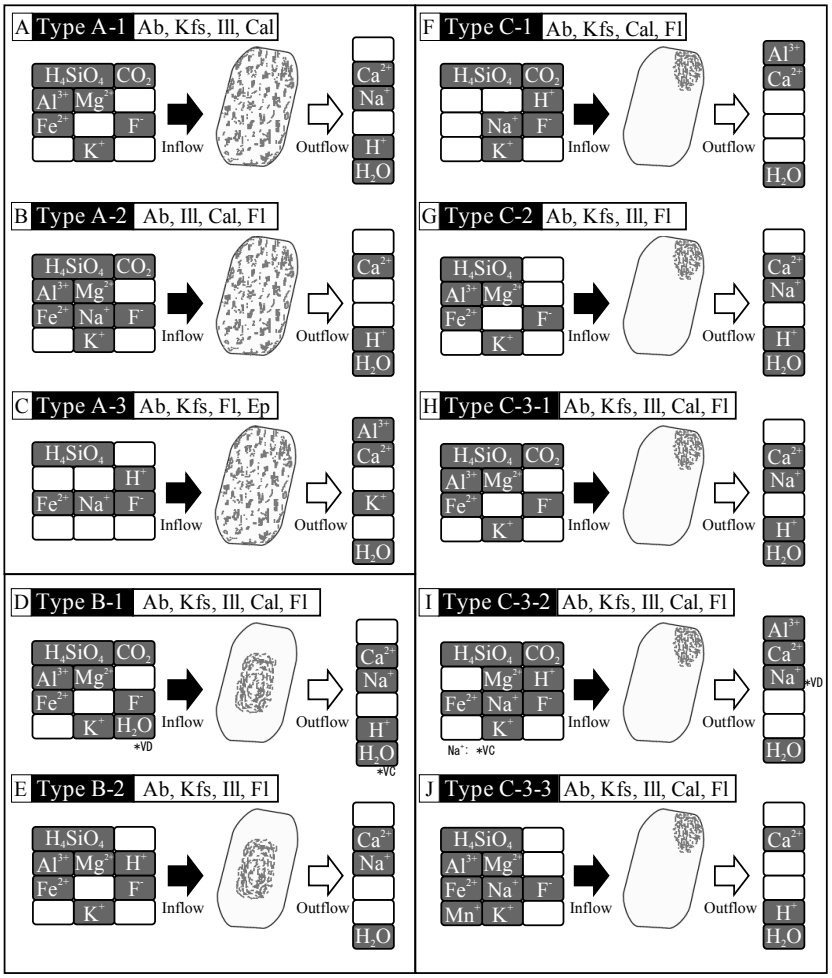

Supplementary Figure S6. Schematic figure showing the inflow and outflow of chemical components through the hydrothermal fluid during the plagioclase alteration.

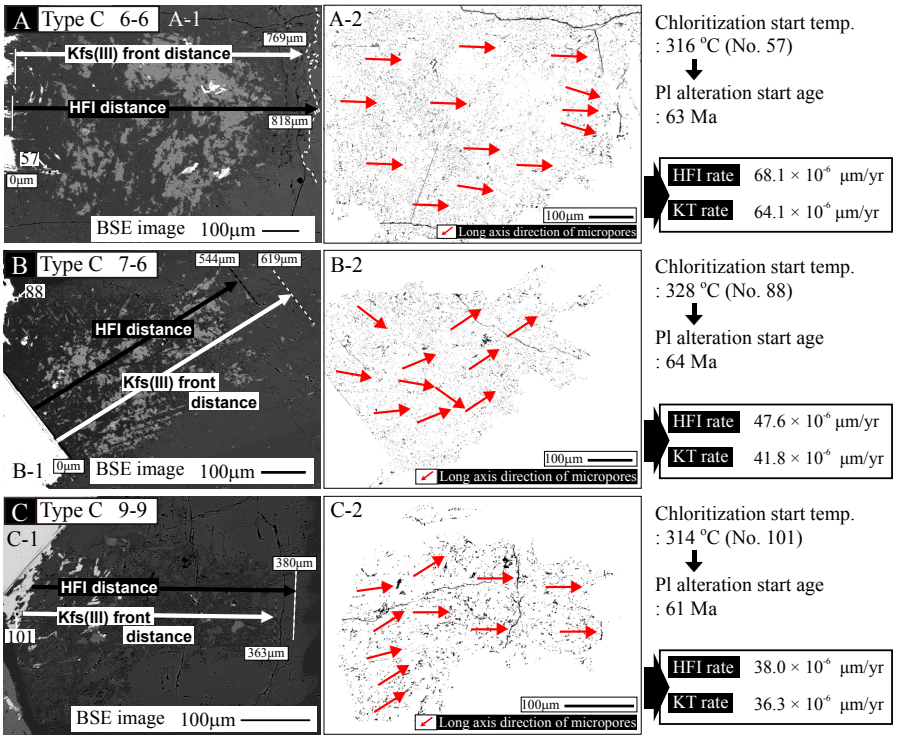

Supplementary Figure S7. Mass transfer rate, including the hydrothermal fluid infiltration rate (HFI rate) and potassium transfer rate (KT rate), through the micropores within plagioclase using samples No. 6-6 (Type C: A), 7-6 (Type C: B), and 9-9 (Type C: C) as examples.